

# Gap state distribution in amorphous hydrogenated silicon carbide films deduced from photothermal deflection spectroscopy

K. Chew, Rusli,<sup>a)</sup> S. F. Yoon, J. Ahn, Q. Zhang, and V. Ligatchev  
*Microelectronics Division, School of Electrical and Electronic Engineering, Nanyang Technological University, Singapore 639798, Republic of Singapore*

E. J. Teo, T. Osipowicz, and F. Watt  
*Research Centre for Nuclear Microscope, Physics Department, National University of Singapore, 10 Kent Ridge Crescent, Singapore 119260*

(Received 29 October 2001; accepted for publication 12 December 2001)

The density of gap states distribution in silicon (Si) rich hydrogenated amorphous silicon carbide ( $a\text{-Si}_{1-x}\text{C}_x\text{:H}$ ) films with varying carbon (C) fraction ( $x$ ) is investigated by the photothermal deflection spectroscopy (PDS). The films are grown using the Electron Cyclotron Resonance Chemical Vapor Deposition (ECR-CVD) technique. By using different methane-to-silane gas flow ratios,  $a\text{-Si}_{1-x}\text{C}_x\text{:H}$  with  $x$  ranging from 0 to 0.36 are obtained. A deconvolution procedure is performed based on a proposed DOS model for these Si rich  $a\text{-Si}_{1-x}\text{C}_x\text{:H}$ . Good fits between the simulated and experimental spectra are achieved, thus rendering support to the model proposed. Deduction of the DOS enables us to obtain various parameters, including the optical gap and the valence band tail width. The fitted mobility gap  $E_g$  is found to be well correlated to the Tauc gap  $E_{\text{tauc}}$  and  $E_{04}$  gap deduced from the optical absorption spectra. A correlation is also seen between the fitted valence band tail width  $E_{vu}$ , the Urbach energy  $E_u$  and the defect density. All these parameters are seen to increase with C alloying. A shift in the defect energy level in the midgap with increasing C incorporation is observed, together with a broadening of the defect distribution and a stronger correlation between the defect bands, which can be accounted for in terms of the influence of C dangling bonds on the deep defect density distribution. © 2002 American Institute of Physics. [DOI: 10.1063/1.1448888]

## I. INTRODUCTION

Hydrogenated amorphous silicon carbide ( $a\text{-Si}_{1-x}\text{C}_x\text{:H}$ ) continues to generate wide interest due to its potential applications in optoelectronics, such as thin film light emitting devices<sup>1</sup> and flat panel displays.<sup>2</sup> Amorphous silicon based solar cells with improved efficiency has been achieved when  $a\text{-Si}_{1-x}\text{C}_x\text{:H}$  is used as the  $p$ -type window layer.<sup>3</sup> These useful applications stem from the tunable optical energy gap and refractive index of  $a\text{-Si}_{1-x}\text{C}_x\text{:H}$ , which can be achieved through changing the C fraction  $x$ , thus allowing the flexibility of tailoring the alloy to specific applications. However, studies have shown that C incorporation also increases the defect density in the pseudogap of  $a\text{-Si}_{1-x}\text{C}_x\text{:H}$  films and critically affects their properties such as doping efficiency, electronic transport, recombination, and width and potential profile of space charge layers in devices.<sup>4,5</sup> Thus it is important to obtain information on the density of the gap states (DOGS) and their energy distribution.

Photothermal deflection spectroscopy (PDS) is a widely used technique for measuring optical absorption and deducing the DOGS distribution in amorphous semiconductors. The strength of PDS lies in that it measures subgap absorption, a process that is closely related to the densities and energy levels of all the defects. It is not constrained by the

Fermi level position, the type of defects and a limited probing energy range in the pseudogap, as encountered in many other techniques such as field effect, capacitance and photoconductivity measurements.<sup>6,7</sup> It has been utilized extensively to deduce the defect density distribution in  $a\text{-Si:H}$ ,<sup>6,8,9</sup> amorphous carbon films,<sup>10</sup> and more recently in diamond.<sup>11</sup> In contrast, comparatively less work have been carried out for  $a\text{-Si}_{1-x}\text{C}_x\text{:H}$ . In this work we apply it to investigate the DOGS distribution within the optical gap of Si rich  $a\text{-Si}_{1-x}\text{C}_x\text{:H}$  films. The films were grown using the electron cyclotron resonance chemical vapor deposition (ECR-CVD) technique, with varying C–Si ratio so as to study the effect of C alloying on the distribution of defect density. The gap state distribution is deduced from the PDS absorption data based on a proposed DOGS model, which describes the defect-induced optical absorption in Si rich  $a\text{-Si}_{1-x}\text{C}_x\text{:H}$ . The analysis involves varying several parameters in the model and a deconvolution procedure to calculate the theoretical absorption spectra, and to fit them to those obtained experimentally. We show that the optical absorption can be well fitted to the experimental data by taking into account optical transitions due to the presence of defect states at the midgap, which is enhanced by C alloying. The nature of the defects and their evolution with C alloying are investigated and analyzed.

<sup>a)</sup>Electronic mail: erusli@ntu.edu.sg

## II. EXPERIMENTAL PROCEDURE

The  $a\text{-Si}_{1-x}\text{C}_x\text{:H}$  samples were grown using the ECR-CVD technique. The details and schematic diagram of the deposition system can be found elsewhere.<sup>12</sup> The microwave power used was 900 W and the upper and lower magnetic coil currents was fixed at 100 and 120 A, respectively. The deposition pressure was maintained at 20 mTorr and no intentional heating was applied. The hydrogen ( $\text{H}_2$ ) flow rate was maintained at 100 sccm, while the gas ratio of methane ( $\text{CH}_4$ ) to silane ( $\text{SiH}_4$ ) was varied to produce films with changing C to Si (C/Si) ratio. The films thicknesses are in the range of 1  $\mu\text{m}$ , measured with a Dektak III surface profiler.

The C fractions  $x$  (C/C+Si) of the films were deduced from Rutherford Backscattering Spectrometry (RBS), using 2 MeV  $\text{H}^+$ . The surface barrier detector was mounted at 20° scattering angle to detect the backscattered particles for the determination of C and Si content in the films. The optical absorption coefficient ( $\alpha$ ) over a wavelength range of 200–900 nm was deduced through the transmittance and reflectance spectra measured using a dual beam Perkin–Elmer Lambda 16 UV-VIS spectrophotometer. The PDS measurements were performed using a conventional setup similar to that found in Ref. 6. The probe beam is a 632.8 nm He–Ne laser, the deflecting medium used is  $\text{CCl}_4$  and the pump beam is 1 kW quartz tungsten halogen lamp focused on the slit of a 1/4-m monochromator. The intensity modulation of the output from the monochromator is accomplished using a mechanical chopper. A low modulation frequency of 10 Hz was adopted to achieve a good signal-to-noise ratio. The deflection of the probe beam was measured by a position detector and fed into a computer-interfaced lock-in amplifier. The amplitude of the PDS signal is then averaged and normalized to the incident light intensity. The scanning range covers photon energies from 1 to 2.8 eV. The spectra at energies lower than 1 eV were very noisy and, therefore, discarded. Various order-sorting filters were used to filter out unwanted diffraction orders. The  $\alpha$  spectra are then calibrated by matching them to those deduced using the UV-VIS spectrophotometry at high photon energies.

## III. DENSITY OF GAP STATES MODEL

The DOS model proposed for  $a\text{-Si}_{1-x}\text{C}_x\text{:H}$  is shown in Fig. 1, which follows closely that for  $a\text{-Si:H}$ . Petrich *et al.*<sup>13</sup> reported that in their Si rich (C content <20 at.%)  $a\text{-Si}_{1-x}\text{C}_x\text{:H}$  films grown using the plasma enhanced chemical vapor deposition (PECVD) technique with source gases  $\text{CH}_4$ ,  $\text{SiH}_4$ , and  $\text{H}_2$ , the alloy forms “amorphous silicon-like” lattices. Investigations on the electronic structure of Si rich  $a\text{-Si}_{1-x}\text{C}_x\text{:H}$  also revealed that the band edges are Si-like.<sup>14</sup> These form the basis for applying the  $a\text{-Si:H}$  model to our Si rich  $a\text{-Si}_{1-x}\text{C}_x\text{:H}$  films. Several reports have shown that the incorporation of a small amount of C into the  $a\text{-Si:H}$  network increases the degree of disorder in the films, causing a broadening of the Urbach tail width and an increase in the defect density, as compared to pure  $a\text{-Si:H}$ .<sup>4,15</sup> The C alloying effect becomes progressively prominent as  $x$  advances, where apart from Si dangling bonds, C dangling

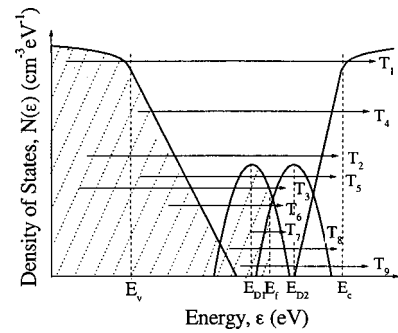


FIG. 1. The proposed density of states (DOS) distribution model for  $a\text{-Si}_{1-x}\text{C}_x\text{:H}$ . The transitions involved are represented by  $T_1$ – $T_9$ .  $T_1$ : Valence band to conduction band,  $T_2$ : Valence band to conduction band tail,  $T_3$ : Valence band to empty defect,  $T_4$ : Valence band tail to conduction band,  $T_5$ : Valence band tail to conduction band tail,  $T_6$ : Valence band tail to empty defect,  $T_7$ : Filled defect to empty defect,  $T_8$ : Filled defect to conduction band tail,  $T_9$ : Filled defect to conduction band.  $E_v$  denotes the valence band edge,  $E_D$  the filled defect band,  $E_f$  the Fermi level,  $U$  the correlation energy and  $E_c$  the conduction band edge. The hatched region represents filled states, while the unshaded region the unfilled states.

bonds are also an increasingly important source of deep defects.<sup>14,16</sup> In our model, the deep defects are assumed to arise mainly from Si dangling bonds, and the effect of C alloying can be accommodated in terms of the different density, distribution and energy levels of the defect states.

Based on the proposed model, the optical transitions that are involved can be divided into three categories, i.e., transitions to the conduction band, to the conduction band tail and to the empty deep defect states, from each of the following: The valence band, the valence band tail and the filled defect states. Therefore, a total of nine transitions are possible, which are labeled  $T_1$  through  $T_9$  as indicated in Fig. 1. These will give rise to a power-law region in the absorption spectra for transitions involving extended states, an exponential (Urbach) edge for transitions related to tail states, and a shoulder region at low absorption energy for transitions involving deep defect states. In our analysis, all the possible transitions will be considered in fitting the experimental absorption coefficient ( $\alpha$ ) spectra.

In the following, the DOS for the conduction band, valence band and gap states are denoted by  $N_k(\epsilon)$ , where the subscript  $k$  denotes the region involved and  $\epsilon$  is the energy level measured with reference to the conduction band edge  $E_c$ , taken to be  $\epsilon=0$ . The magnitude of the valence band edge  $E_v$ , therefore, represents the mobility gap  $E_g$ . The DOS for the extended states in the conduction band  $N_c(\epsilon)$  and valence band  $N_v(\epsilon)$  are described by the following parabolic expressions<sup>17</sup>

$$N_c(\epsilon) = N_{co}(\epsilon + \epsilon_o)^{1/2}, \quad (1)$$

$$N_v(\epsilon) = N_{vo}|(\epsilon - E_v - \epsilon_o)|^{1/2}, \quad (2)$$

where  $N_{co}$  and  $N_{vo}$  are the free electron values in the extended states and  $\epsilon_o$  is a constant that reduces the abruptness of  $N_c(\epsilon)$  and  $N_v(\epsilon)$  at the mobility edges.

The DOS of the band tails are represented by two exponentially decaying functions

TABLE I. Comparison of the parameters obtained from experimental optical absorption spectra and deduced from the PDS measurements based on the proposed DOS model.  $E_{\text{tauc}}$  and  $E_{04}$  are the optical gaps derived from the Tauc's relation and at  $\alpha=10^4 \text{ cm}^{-1}$ , respectively, and  $E_u$  is the Urbach energy.  $E_g$  is the fitted mobility gap,  $E_{vu}$  the valence band tail width,  $E_{D1}$  the  $D^0$  defect peak energy with reference to the conduction band edge,  $W$  and  $A$  are the width and density of the defect distributions, respectively, and  $U$  is the correlation energy between  $D^0$  and  $D^-$ .

Carbon fraction, $x$	Derived from the experimental optical absorption spectra			Deduced from PDS measurements based on the proposed DOS model					
	$E_{\text{tauc}}$ (eV)	$E_{04}$ (eV)	$E_u$ (meV)	$E_g$ (eV)	$E_{vu}$ (meV)	$E_{D1}$ (eV)	$W$ (eV)	$A$ ( $\times 10^{17} \text{ cm}^{-3}$ )	$U$ (eV)
0	1.92	2.17	92	2.00	84	-1.05	0.09	2.17	0.29
0.18	1.93	2.20	105	2.05	92	-1.00	0.10	2.30	0.30
0.22	1.93	2.21	109	2.06	100	-0.97	0.09	4.22	0.29
0.36	2.11	2.45	134	2.36	143	-1.29	0.17	8.64	0.60

$$N_{cbt}(\epsilon) = N_{cbto} \exp\left(\frac{\epsilon}{E_{cu}}\right), \quad (3)$$

$$N_{vbt}(\epsilon) = N_{vbto} \exp\left(\frac{-(\epsilon - E_v)}{E_{vu}}\right), \quad (4)$$

where  $N_{cbto}$  and  $N_{vbto}$  are the conduction and valence band tail densities at the respective mobility edges, and  $E_{cu}$  and  $E_{vu}$  are, respectively, the conduction and valence band tail widths.

For our Si rich  $a\text{-Si}_{1-x}\text{C}_x\text{:H}$ , it is though that Si dangling bonds are the major contributor to the defect states deep in the energy gap, arising from  $\sigma$  defects which are isolated threefold coordinated sites, as in  $a\text{-Si:H}$ . There is a general agreement that for intrinsically undoped  $a\text{-Si:H}$ , the midgap densities can be ascribed to a distribution of states made up of neutral singly occupied dangling bonds,  $D^0$ . It has a positive correlation energy  $U$ , which is the energy required to place a second electron on the singly occupied defect states, to create negatively charged dangling bonds,  $D^-$ . Therefore, the  $D^-$  states are higher in energy than  $D^0$  states by  $U$ , and these are situated above and below the midgap respectively.<sup>18-20</sup> The two distributions can be represented by two Gaussian distributions with densities  $N_{D1}$  (for  $D^0$  states) and  $N_{D2}$  (for  $D^-$  states) centered at  $\epsilon = E_{D1}$  and  $\epsilon = E_{D1} + U = E_{D2}$ , respectively,

$$N_{D1}(\epsilon) = \frac{A}{W\sqrt{2\pi}} \exp\left(\frac{-(\epsilon - E_{D1})^2}{2W^2}\right), \quad (5)$$

$$N_{D2}(\epsilon) = \frac{A}{W\sqrt{2\pi}} \exp\left(\frac{-(\epsilon - E_{D1} - U)^2}{2W^2}\right). \quad (6)$$

In the above,  $A/(W\sqrt{2\pi})$  is the peak amplitude, and  $W$  is known as the width, or more specifically the root-mean square deviation from the mean value of the distribution.<sup>21-23</sup> The full width at half maximum (FWHM) of the distribution is given by  $2W\sqrt{2 \ln 2}$ , and the integrated area is given by  $A$ , which also represents the overall defect densities.<sup>24</sup> It should be noted that this model applies only to Si rich samples. In C rich samples, the model will have to be modified to account for the presence of  $\pi$  states in threefold coordinated ( $sp^2$ ) sites of C.<sup>14</sup>

For electronic transitions in amorphous semiconductors, energy conservation is observed, but momentum conservation is relaxed. This allows all pairs of states separated by the

same photon energy to contribute equally to  $\alpha$ . As such, within the one-electron approximation and following the Velicky summation rule, the optical absorption coefficient  $\alpha(h\nu)$  at a photon energy  $h\nu$ , for transitions between the energy levels  $\epsilon$  and  $\epsilon + h\nu$ , can be represented by the convolution of the continuous densities of initial (filled)  $N_i(\epsilon)$  states and final (unfilled)  $N_f(\epsilon + h\nu)$  states.<sup>25,26</sup> It can be written as

$$\alpha(h\nu) = \frac{M}{h\nu} \int N_i(\epsilon) f(\epsilon) \cdot N_f(\epsilon + h\nu) [1 - f(\epsilon + h\nu)] d\epsilon, \quad (7)$$

where  $f(\epsilon)$  and  $f(\epsilon + h\nu)$  are the Fermi-Dirac distribution functions at the initial and final state energies, respectively. The prefactor  $M$  is proportional to the dipole moment matrix elements.<sup>25</sup> By substituting the different initial and final states using Eqs. (1)-(6) and summing up all the contributions, the theoretical absorption spectra can be obtained.

#### IV. RESULTS AND DISCUSSIONS

The parameters that are kept constant in the deconvolution procedure are as follows. In Eqs. (1) and (2),  $N_{co} = N_{vo} = 6.7 \times 10^{21} \text{ cm}^{-3} \text{ eV}^{-3/2}$  following Refs. 26 and 27, and  $\epsilon_o$  is fixed at 0.0223 eV to yield  $1 \times 10^{21} \text{ cm}^{-3} \text{ eV}^{-1}$  for both  $N_c(\epsilon = 0)$  and  $N_v(\epsilon = E_v)$  at the mobility edges.<sup>17,28,29</sup> Naturally,  $N_{cbto}$  and  $N_{vbto}$  in Eqs. (3) and (4) are set to  $1 \times 10^{21} \text{ cm}^{-3} \text{ eV}^{-1}$  for a continuity in the DOS between the extended and tail states at the mobility edges. The Fermi level is assumed to be very close to midgap,  $E_f \sim 0.9 \text{ eV}$  below  $E_c$  for  $x=0$  since the film is intrinsically undoped.<sup>20,21,29</sup> Note that the fitted mobility gap  $E_g$  of this sample is about 2 eV, see Table I. We assume that  $E_f$  remains unchanged across the samples with varying  $x$ , which is supported by the results of Robertson,<sup>14</sup> where it was shown that  $E_f$  moves in parallel with  $E_c$  for small  $x$  ( $< 0.4$ ). In Si rich  $a\text{-Si}_{1-x}\text{C}_x\text{:H}$ , the band edges are Si-like,<sup>14</sup> thus it is expected that their characteristics are similar to  $a\text{-Si:H}$ , where the tail width is wider at the valence band than the conduction band. As a result, the valence band tail states are expected to be the major contributor to the exponential region of the  $\alpha$  spectra. In order to deduce the valence band tail width  $E_{vu}$ , we have taken  $E_{cu}$  to be a constant with  $E_{cu} = 0.03 \text{ eV}$ , which is within the experimental range.<sup>17,30,31</sup> In-

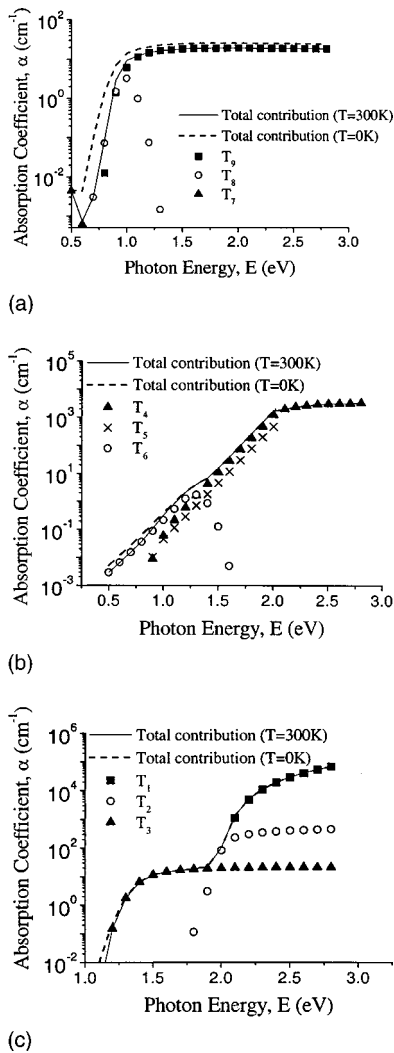


FIG. 2. Breakdown of the contributions from all the nine possible transitions considered. The  $a\text{-Si}_{1-x}\text{C}_x\text{:H}$  sample with  $x=0.22$  is used in this example. (a) Contribution from the filled defects, (b) contributions from valence band tail, and (c) contributions from the valence band.

deed, it will be shown that  $E_{cu}$  is much smaller than the fitted  $E_{vu}$  (see Fig. 7 or Table I), which thus justifies the assumption made.

In Eq. (7),  $M$  is taken to be a constant for all the transitions regardless of the photon energy. Strictly speaking, among the optical transitions, those involving localized to localized states will have smaller  $M$ . If these transitions were to have any significant contribution, it will only occur for  $h\nu < 1$  eV (see Fig. 3). Since we are only considering experimental data for  $h\nu > 1$  eV, therefore, our assumption of a constant  $M$  will have no effect on the fitting process. Indeed, it is experimentally confirmed by Jackson *et al.* that in  $a\text{-Si:H}$ , the spectral dependence of the dipole moment matrix elements are weak (within a factor of 2) in the subgap and above the mobility edges, up to  $\sim 3.4$  eV.<sup>32</sup> For the two defect distributions given in Eqs. (5) and (6), as a first approximation, they are assumed to be equal in their heights and widths. A similar approximation has been made for the gap state defect distributions in  $a\text{-Si:H}$  and in diamond using the PDS technique.<sup>11,24,33</sup> However, it is also noted that there

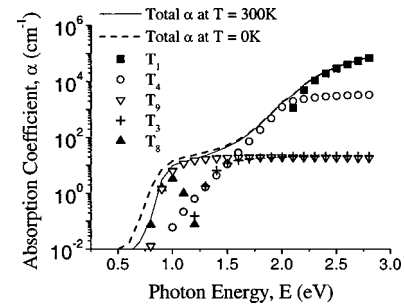


FIG. 3. The absorption spectrum deduced for the sample with  $x=0.22$ , taking into account all the nine possible transitions. From Figs. 2(a)–2(c), the major transitions contributing to  $\alpha$  are singled out and shown here.

exist reports where these are assumed to be different.<sup>8,34</sup> Summing up, a total of seven parameters are to be fitted. These include the prefactor  $M$ , the mobility gap  $E_g (=E_c - E_v)$ , the valence band tail width  $E_{vu}$ , the width  $W$  and the height of the defect distributions (which also gives the defect density  $A$ ) and their peak energy levels,  $E_{D1}$  and  $E_{D2} = E_{D1} + U$ .

To clearly understand the contributions of the various optical transitions to the  $\alpha$  spectra, the absorptions arising from each transition are illustrated in detail in Fig. 2, for the sample with  $x=0.22$ . Figs. 2(a)–2(c) depict the absorption spectra due to transitions from the filled defect, valence band tail and valence band states respectively to the various higher energy states. Figure 3 shows the overall fitted curve, clearly detailing the dominant transitions that shape the  $\alpha$  spectra. In particular, transitions to the conduction band are the most significant due to its high density of empty states available. Transitions from the filled defect states to the conduction band tail at around  $h\nu = 1$  eV ( $T_8$ ) and from the valence band to empty defect states ( $T_3$ ) at around  $h\nu = 1.5$  eV are also affecting the overall spectra. In fitting the spectra, it is noted that the width of the Gaussian distribution  $W$  and correlation energy  $U$  are mainly reflected in the absorption corresponding to  $T_3$  and  $T_9$ . We obtained  $W \sim 0.1$  eV,  $U \sim 0.3$  eV and  $E_{D1} \sim 1$  eV below  $E_c$  for all samples (except for  $x=0.36$ , which will be discussed in the next section) which are similar to the values observed for a typical  $a\text{-Si:H}$ .<sup>17,19–21,35</sup> This gives support to the assertion that the defect states in Si rich  $a\text{-Si}_{1-x}\text{C}_x\text{:H}$  arise mainly from Si dangling bonds, as in the case of  $a\text{-Si:H}$ . In our calculation,  $T$  is taken to be 300 K, the temperature at which the measure-

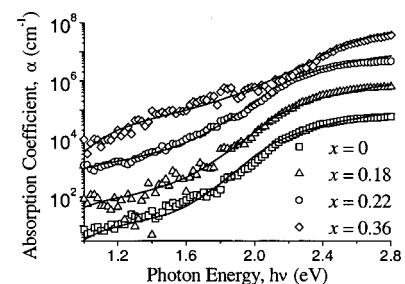


FIG. 4. Experimental (symbols) and calculated (solid lines) PDS spectra based on the DOS model proposed for  $a\text{-Si}_{1-x}\text{C}_x\text{:H}$  with varying composition  $x$ . The spectra are displaced vertically by a decade for clarity.

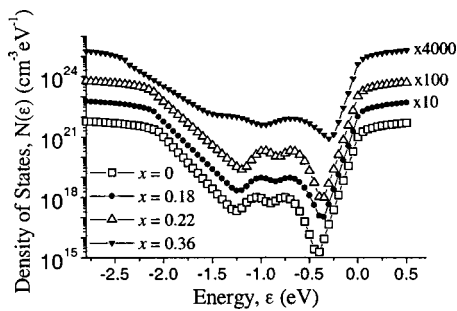


FIG. 5. The density of states distributions calculated based on the best-fitted parameters obtained in the PDS spectra deconvolution procedure.

ments are performed. A difference is observed if the zero temperature approximation is used, especially at lower photon energies, as elucidated in Figs. 2 and 3, (compare the solid and the dotted lines). Thus using  $T = 300$  K in  $f(\epsilon)$  will lead to more accurate results.

In the deconvolution procedure, the best-fitted parameters obtained for all the samples with  $x$  varying from 0 to 0.36 are summarized in Table I. The theoretical PDS spectra calculated based on these parameters are shown in Fig. 4, together with the corresponding experimental spectra. The good agreement between them as seen provides further support to the application of the DOGS model to Si rich  $a$ -Si<sub>1-x</sub>C<sub>x</sub>:H. The slight deviation observed at large photon energies ( $h\nu > 2.6$  eV) is attributed to the parabolic band edge assumption made [see Eqs. (1) and (2)], which may not be valid for  $h\nu$  that exceeds far beyond the optical gap (see Fig. 6 or Table I). The DOS distributions constructed from the best-fitted parameters for all the samples are shown in Fig. 5, with the origin of the energy scale  $\epsilon = 0$  set at the conduction band edge  $E_c$ .

Besides the fitted parameters, some other parameters deduced directly from the experimental absorption spectra are also shown in Table I for comparison. The best fitted  $E_g$  increases with  $x$ , and as shown in Fig. 6, have values that are in between  $E_{\text{tauc}}$  and  $E_{04}$ , which are, respectively, the Tauc gap and the optical gap at which  $\alpha = 10^4 \text{ cm}^{-1}$ . We noticed that using  $E_{04}$  for  $E_g$  in the PDS spectra fitting will result in a too drastic decrease at the shoulder of the power law region of the  $\alpha$  curve, whereas using  $E_{\text{tauc}}$  will produce a curve which is broader than what is obtained experimentally. In

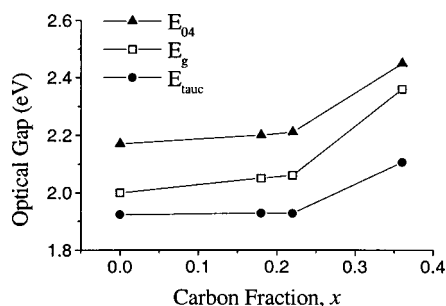


FIG. 6. The optical gaps of  $a$ -Si<sub>1-x</sub>C<sub>x</sub>:H as a function of  $x$ .  $E_g$  is the fitted mobility gap,  $E_{\text{tauc}}$  is the Tauc gap and  $E_{04}$  the optical gap at which  $\alpha = 10^4 \text{ cm}^{-1}$ . The latter two parameters are deduced from the optical absorption spectra.

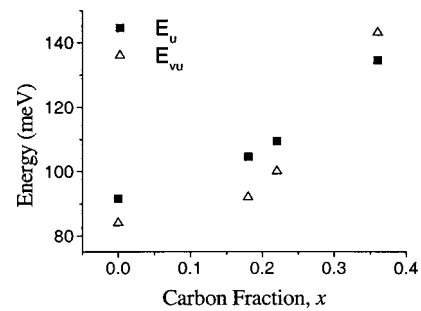


FIG. 7. Correlation between the Urbach energy  $E_u$  and the fitted valence band tail width  $E_{vu}$  with carbon fraction  $x$ .

amorphous semiconductors, there is no distinct demarcation energy level to define the energy gap. Therefore,  $E_g$  obtained from the PDS fitting can be interpreted as an approximate average value between  $E_{\text{tauc}}$  and  $E_{04}$ , and just like the two, also represents an indicative value of the optical gap.

The valence band tail width  $E_{vu}$  found from the fitting procedure are shown in Fig. 7. It correlates well with the Urbach energy  $E_u$  deduced from the exponential region of the  $\alpha$  spectra using the equation  $\alpha = \alpha_0 \exp(h\nu/E_u)$ . The band tail states are considered to be related to weak Si-Si bonds, arising from the strain present in the disordered network.<sup>36</sup> These are enhanced with C alloying due to more structural disorder introduced as a result of the different bond lengths and bond strengths of C and Si.<sup>37</sup> Hence  $E_u$  and  $E_{vu}$  are expected to increase with C alloying, as confirmed in Fig. 7.

The defect density  $A$  deduced for the films are found to increase with  $x$ , as can be seen in Fig. 8. This reflects larger dangling bond defect densities, concomitant with an increase in the valence band tail slope  $E_{vu}$  as discussed earlier. The variation in the density of defect and band tail states can be explained by generalizing the weak bond to dangling bond conversion model of Stutzman.<sup>38</sup> This model attributes tail states in  $a$ -Si:H to weak bonds, which when lie beyond a certain demarcation energy above the valence band edge,

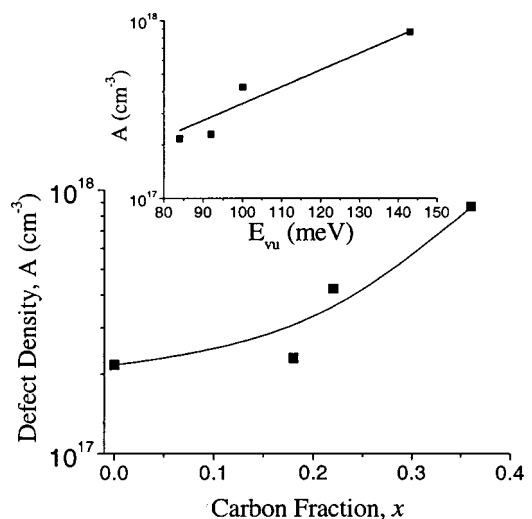


FIG. 8. The dependence of defect density  $A$  on the carbon fraction  $x$ . Inset: the relation of  $A$  with the fitted valence band tail width  $E_{vu}$ . The solid line shows the correlation between  $A$  and  $E_{vu}$ .

tend to convert to dangling bonds by bond breaking so that they can minimize their energy locally. Therefore, it is expected that a wider valence band tail will give rise to a higher defect density. Indeed, if we plot the defect density  $A$  against  $E_{vu}$ , as shown in the inset of Fig. 8, a correlation can be seen, where  $\alpha \propto \exp(E_{vu}/46 \text{ meV})$ . This suggests the dangling bonds are closely related to the disorder-induced fields and strains that are responsible for controlling the width of the valence band tail states.

The peak energy of the midgap defect distribution  $E_{D1}$  for  $x \leq 0.22$  was found to be located at  $\sim 1 \text{ eV}$  below  $E_c$ . However, for  $x = 0.36$ , a good fit can only be obtained if  $E_{D1}$  is shifted to  $\sim 1.3 \text{ eV}$  below  $E_c$ . At the same time,  $W$  and  $U$  are increased significantly. This shift away from  $E_c$  is also observed in the steady-state optical modulation spectroscopy (OMS) study of defect distributions in  $a\text{-Si}_{1-x}\text{C}_x\text{:H}$  deposited by the conventional r.f. glow discharge technique.<sup>39</sup> Similar observations on the change in  $W$  and  $U$  have been reported by Demichelis *et al.* in their PDS study of PECVD grown Si rich  $a\text{-Si}_{1-x}\text{C}_x\text{:H}$ . Through a derivative procedure, they deduced that  $U$  increases from  $\sim 0.35 \text{ eV}$  to  $\sim 0.6 \text{ eV}$ , while  $W$  widens to  $\sim 0.16 \text{ eV}$  from  $\sim 0.08 \text{ eV}$ , when  $x$  is increased from 0 to 0.24.<sup>34</sup> In the study of the effects of C implantation on the DOS of  $n$ -type  $a\text{-Si:H}$  grown with glow-discharge method, profiling of the subgap DOS with capacitance measurements show no evidence of impurity-related defect band with increasing C dose, but a significant broadening of the Si dangling bond Gaussian defect band by  $\sim 0.05 \text{ eV}$  is found, in good agreement with what is observed here.<sup>40</sup> These observations reflect a change in the origin and the nature of the deep defect states, and are attributed to the increased incorporation of C in the film. As  $x$  increases, the C dangling bonds affect the deep defect states distribution originated from Si dangling bonds. The significance of C dangling bonds is supported by calculations performed for the density of defects in  $a\text{-Si}_{1-x}\text{C}_x\text{:H}$ .<sup>14,41</sup> As evidenced from ESR (electron spin resonance) measurements,<sup>16</sup> C alloying in  $a\text{-Si:H}$  produces resonance  $g$  values between that of Si ( $g = 2.0055$ ) and C ( $g = 2.003$ ), indicating that the spin densities are made up of Si and C singly occupied dangling bonds,  $\text{Si}_3^0$  and  $\text{C}_3^0$ . Here the subscripts represent the coordination number and the superscripts represent the charge state, with symbols + for positive, - for negative and 0 for neutral. On the other hand, LESR (light induced electron spin resonance) measurements<sup>42,43</sup> found that, in addition to the neutral dangling bonds, the spin densities are also contributed by charged defects of Si and C. Owing to the higher electronegativity of C, the  $\text{Si}_3$  level will lie above the  $\text{C}_3$  level, and there will be a charge transfer to give C charged defects with a configuration  $\text{C}_3^-$  and Si charged defects  $\text{Si}_3^+$ .<sup>14</sup> The  $\text{Si}_3$  level is repelled upwards as C is introduced into Si while the  $\text{C}_3$  level is repelled downwards as Si is introduced into C. If  $\text{Si}_3$  outnumbered  $\text{C}_3$  centers, as in Si rich alloy, this will produce  $\text{Si}_3^+$ ,  $\text{Si}_3^0$  and  $\text{C}_3^-$  centers, where  $\text{C}_3^-$  is repelled downwards towards  $E_v$  while  $\text{Si}_3^+$  is repelled upwards towards  $E_c$  by the interaction between the Si and C atoms. It is probable that at larger  $x$ , the increasing number of defect states associated with  $\text{C}_3^-$  accounts for the observed shift of the defect level  $E_{D1}$  further away from  $E_c$ .

A large  $U$  observed implies there exists a strong Coulomb repulsion and the compensation by lattice relaxation is weak.<sup>44,45</sup> This is probably the result of the presence of  $\text{C}_3^-$  centers below  $E_f$ , which causes the  $D^-$  level to shift further away from the  $D^0$  level due to Coulomb repulsion. The broadening of the Gaussian distribution may also be attributed to these changes in the dangling bond environment.

## V. CONCLUSION

We have studied the gap state distribution of Si rich  $a\text{-Si}_{1-x}\text{C}_x\text{:H}$  ( $0 \leq x \leq 0.36$ ) by means of PDS measurements. Good fits are obtained between the calculated and experimental spectra, which render support to the DOS model proposed for such films. Though the model follows closely that for  $a\text{-Si:H}$  where the deep defects are ascribed to Si dangling bonds, it is able to reflect the changes of the distributions due to C alloying. Through a deconvolution procedure, we are able to deduce several parameters: The mobility gap  $E_g$ , the valence band tail width  $E_{vu}$ , the density of gap states  $A$  and their distributions within the mobility gap, as described by their peak energy levels, their widths  $W$  and the correlation energy  $U$  between them. It is found that the fitted mobility gap  $E_g$  is well correlated with the optically deduced Tauc gap  $E_{\text{tauc}}$  and  $E_{04}$ , and the fitted valence band tail width  $E_{vu}$  with the Urbach energy  $E_u$ . All these parameters are seen to increase with C alloying. A correlation is also observed between  $E_{vu}$  and the defect densities which is discussed in terms of the increased disorder in the films with C incorporation. A shift in the defect peak energy  $E_{D1}$  towards the valence band is noted when  $x$  reaches 0.36, together with a broadening of  $W$  and  $U$ , which can be explained in terms of the influence of C dangling bonds on the deep defect density distribution.

<sup>1</sup> Y. Hamakawa, D. Kruangam, T. Toyama, M. Yoshimi, S. Paasche, and H. Okamoto, *Optoelectron.-Devices Technol.* **4**, 281 (1989).

<sup>2</sup> Y. Tawada, K. Tsuge, M. Kondo, H. Okamoto, and Y. Hamakawa, *J. Appl. Phys.* **53**, 5273 (1982).

<sup>3</sup> P. G. LeComber, *J. Non-Cryst. Solids* **115**, 1 (1989).

<sup>4</sup> J. P. Conde, V. Chu, M. F. de Silva, S. Arekat, A. Fedorov, M. N. Berberan-Santos, F. Giorgis, and C. F. Pirri, *J. Appl. Phys.* **85**, 3327 (1999).

<sup>5</sup> A. Desalvo, F. Giorgis, C. F. Pirri, E. Tresso, P. Rava, R. Galloni, R. Rizzoli, and C. Summonte, *J. Appl. Phys.* **81**, 7973 (1997).

<sup>6</sup> N. M. Amer and W. B. Jackson, in *Semiconductors and Semimetals Vol. 21B*, edited by J. I. Pankove (Academic, Florida, 1984), Chap. 3, and references thereof.

<sup>7</sup> G. Moddel, D. A. Anderson, and W. Paul, *Phys. Rev. B* **22**, 1918 (1980).

<sup>8</sup> G. Amato and F. Fizzotti, *Phys. Rev. B* **45**, 14108 (1992).

<sup>9</sup> F. Leblance, Y. Maeda, K. Onisawa, and T. Minemura, *Phys. Rev. B* **50**, 14613 (1994).

<sup>10</sup> D. Dasgupta, F. Demichelis, C. F. Pirri, and A. Tagliaferro, *Phys. Rev. B* **43**, 2131 (1991).

<sup>11</sup> M. Nesladek, K. Meykens, and L. M. Stals, *Phys. Rev. B* **54**, 5552 (1996).

<sup>12</sup> Rusli, S. F. Yoon, H. Yang, Q. Zhang, J. Ahn, and Y. L. Fu, *J. Vac. Sci. Technol. A* **16**, 572 (1998).

<sup>13</sup> M. A. Petrich, K. K. Gleason, and J. A. Reimer, *Phys. Rev. B* **36**, 9722 (1987).

<sup>14</sup> J. Robertson, *Philos. Mag.* **B 66**, 615 (1992).

<sup>15</sup> V. Chu, J. P. Conde, J. Jarego, P. Brogueira, J. Rodriguez, N. Banadas, and J. C. Soares, *J. Appl. Phys.* **78**, 3164 (1995).

<sup>16</sup> C. Palsule, S. Gangopadhyay, D. Cronauer, and B. Schroder, *Phys. Rev. B* **48**, 10804 (1993).

<sup>17</sup> H. Curtins and M. Favre, in *Amorphous Silicon and Related Materials Vol. A*, edited by H. Fritzsche (World Scientific, Singapore, 1988), p. 329.

- <sup>18</sup>F. Wang and R. Schwarz, Phys. Rev. B **52**, 14586 (1995).
- <sup>19</sup>K. Winer, Phys. Rev. Lett. **63**, 1487 (1989).
- <sup>20</sup>M. Gunes, C. R. Wronski, and T. J. McMahon, J. Appl. Phys. **76**, 2260 (1994).
- <sup>21</sup>M. J. Powell and S. C. Deane, Phys. Rev. B **48**, 10815 (1993).
- <sup>22</sup>J. W. Goodman, in *Statistical Optics* (Wiley, New York, 1985), p. 34.
- <sup>23</sup>H. C. Ohanian, in *Principles of Quantum Mechanics* (Prentice-Hall, New Jersey, 1990), p. 40.
- <sup>24</sup>J. Kocka, M. Vanecek, and A. Triska, in *Amorphous Silicon and Related Materials*, edited by H. Fritzsche (World Scientific, Singapore, 1989), p. 305.
- <sup>25</sup>G. D. Cody, in *Semiconductors and Semimetals*, edited by J. I. Pankove (Academic, Florida, 1984), Chap. 2.
- <sup>26</sup>G. A. N. Connell, in *Amorphous Semiconductors*, Topics in Applied Physics Vol. 36, edited by M. H. Brodsky (Springer-Verlag, Germany, 1979), Chap. 4.
- <sup>27</sup>M. Vanecek, J. Kocka, J. Stuchlik, Z. Kozisek, O. Stika, and A. Triska, Sol. Energy Mater. **8**, 411 (1983).
- <sup>28</sup>J. M. Asensi and J. Andreu, Phys. Rev. B **47**, 13295 (1993).
- <sup>29</sup>M. Gunes and C. R. Wronski, Appl. Phys. Lett. **61**, 678 (1992).
- <sup>30</sup>M. Gunes and C. R. Wronski, J. Appl. Phys. **81**, 3526 (1997).
- <sup>31</sup>S. Lee, M. Gunes, C. R. Wronski, N. Maley, and M. Bennett, Appl. Phys. Lett. **59**, 1578 (1991).
- <sup>32</sup>W. B. Jackson, S. M. Kelso, C. C. Tsai, J. W. Allen, and S.-J. Oh, Phys. Rev. B **31**, 5187 (1985).
- <sup>33</sup>G. Amato and F. Giorgis, J. Appl. Phys. **74**, 3956 (1993).
- <sup>34</sup>F. Demichelis, G. Crovini, F. Giorgis, C. F. Pirri, E. Tresso, G. Amato, H. Herremans, W. Grevenadonk, and P. Rava, J. Non-Cryst. Solids **164–166**, 1016 (1993).
- <sup>35</sup>J. Kocka, J. Stuchlik, M. Stutzmann, L. Chen, and J. Tauc, Phys. Rev. B **47**, 13283 (1993).
- <sup>36</sup>T. Unold, J. Hautala, and J. D. Cohen, Phys. Rev. B **50**, 16985 (1994).
- <sup>37</sup>M. A. El Khakani, D. Guay, M. Chaker, and X. H. Feng, Phys. Rev. B **51**, 4903 (1995).
- <sup>38</sup>R. A. Street and K. Winer, Phys. Rev. B **40**, 6236 (1989).
- <sup>39</sup>H. Herremans, W. Grevenadonk, R. A. C. M. M. van Swaaij, W. G. J. H. M. van Sark, A. J. M. Berntsen, W. M. Arnold Bik, and J. Bezemer, Philos. Mag. B **66**, 796 (1992).
- <sup>40</sup>C. E. Michelson and J. D. Cohen, Phys. Rev. B **41**, 1529 (1990).
- <sup>41</sup>F. Alvarez and M. Sebastini, J. Appl. Phys. **71**, 5969 (1992).
- <sup>42</sup>X. Xu, H. Sasaki, A. Morimoto, M. Kumeda, and T. Shimizu, Phys. Rev. B **41**, 10049 (1990).
- <sup>43</sup>T. Shimizu, H. Kidoh, A. Morimoto, and M. Kumeda, Jpn. J. Appl. Phys. Part I **28**, 586 (1989).
- <sup>44</sup>R. A. Street, in *Hydrogenated Amorphous Silicon* (Cambridge University Press, Great Britain, 1991), p. 99.
- <sup>45</sup>D. Adler, in *Semiconductors and Semimetals*, edited by J. I. Pankove (Academic, Florida, 1984), Chap. 14.